

# Ising magnetism and ferroelectricity in $\text{Ca}_3\text{CoMnO}_6$

Hua Wu,<sup>1</sup> T. Burnus,<sup>1</sup> Z. Hu,<sup>1</sup> C. Martin,<sup>2</sup> A. Maignan,<sup>2</sup> J. C. Cezar,<sup>3</sup>  
A. Tanaka,<sup>4</sup> N. B. Brookes,<sup>3</sup> D. I. Khomskii,<sup>1</sup> and L. H. Tjeng<sup>1</sup>

<sup>1</sup>*II. Physikalisches Institut, Universität zu Köln, Zùlpicher Str. 77, 50937 Köln, Germany*

<sup>2</sup>*Laboratoire CRISMAT, UMR 6508 CNRS ENSICAEN, 14050 Caen, France*

<sup>3</sup>*European Synchrotron Radiation Facility, Boîte Postale 220, 38043 Grenoble Cédex, France*

<sup>4</sup>*Department of Quantum Matter, ADMS, Hiroshima University, Higashi-Hiroshima 739-8530, Japan*

(Dated: February 10, 2022)

The origin of both the Ising chain magnetism and ferroelectricity in  $\text{Ca}_3\text{CoMnO}_6$  is studied by *ab initio* electronic structure calculations and x-ray absorption spectroscopy. We find that  $\text{Ca}_3\text{CoMnO}_6$  has the alternate trigonal prismatic  $\text{Co}^{2+}$  and octahedral  $\text{Mn}^{4+}$  sites in the spin chain. Both the  $\text{Co}^{2+}$  and  $\text{Mn}^{4+}$  are in the high spin state. In addition, the  $\text{Co}^{2+}$  has a huge orbital moment of  $1.7 \mu_B$  which is responsible for the significant Ising magnetism. The centrosymmetric crystal structure known so far is calculated to be unstable with respect to exchange striction in the experimentally observed  $\uparrow\uparrow\downarrow$  antiferromagnetic structure for the Ising chain. The calculated inequivalence of the Co-Mn distances accounts for the ferroelectricity.

PACS numbers: 71.20.-b, 78.70.Dm, 71.70.-d, 71.27.+a

Among a variety of multiferroic materials discovered so far [1, 2], ferroelectric Ising chain magnet  $\text{Ca}_3\text{CoMnO}_6$  is quite unique, because the ferroelectricity (FE) is driven by exchange striction in a collinear Ising spin chain consisting of the charge ordered transition-metal ions [3]. The spin chain has the alternate trigonal prismatic and octahedral sites [3, 4]. Special  $\uparrow\uparrow\downarrow$  antiferromagnetic (AF) structure is detected in  $\text{Ca}_3\text{CoMnO}_6$  below  $T_N \approx 13$  K by neutron diffraction. However, the measured magnetic moment of  $0.66 \mu_B/\text{Co}$  and  $1.93 \mu_B/\text{Mn}$  is much smaller than the expected one of the normal high-spin (HS)  $\text{Co}^{2+}$  ( $S=3/2$ ) and  $\text{Mn}^{4+}$  ( $S=3/2$ ). This led Choi *et al.* to a conclusion that the  $\text{Co}^{2+}$  is (surprisingly) in a low-spin (LS) state [3]. In contrast, the effective magnetic moment of  $\mu_{\text{eff}}=5.8\text{--}6.0 \mu_B$  per formula unit (f.u.), extracted from magnetic susceptibility measurements above  $T_N$  [4, 5], suggests that both  $\text{Co}^{2+}$  and  $\text{Mn}^{4+}$  are in a HS state. Thus there is an apparent controversy between those data, and the problem concerning the spin state of, in particular,  $\text{Co}^{2+}$  ions seems to be still unsolved. Another important question is to understand the nature of the Ising magnetism and of the resulting exchange striction, which are apparently crucial for the appearance of FE in  $\text{Ca}_3\text{CoMnO}_6$ . To this end, we carried out *ab initio* electronic structure calculations and x-ray absorption spectroscopy (XAS). We address the important issues including the Co/Mn site preference, their charge/spin/orbital states, the origin of the Ising magnetism, and the exchange striction.

Our *ab initio* calculations were performed by using the full-potential augmented plane waves plus local orbital method (Wien2k code) [6]. We took the experimental centrosymmetric structure data of the rhombohedral lattice ( $R\bar{3}c$ ) which has in a hexagonal setting the lattice constant  $a=9.1314 \text{ \AA}$  and  $c=10.5817 \text{ \AA}$  [4, 7]. The calculations were done for different magnetic structures

( $\uparrow\uparrow\uparrow$ ,  $\uparrow\uparrow\downarrow$ ,  $\uparrow\downarrow\downarrow$ , and  $\uparrow\downarrow\uparrow$  orderings in the Co-Mn-Co-Mn chains). To study the exchange striction effect, we investigated the effect of internal atomic relaxation allowing the inversion symmetry to be broken in the  $\uparrow\uparrow\downarrow$  spin chain, as discussed below. The muffin-tin sphere radii are chosen to be 2.4, 2.1 and 1.4 Bohr for Ca, Co/Mn and O atoms, respectively. The cut-off energy of 16 Ryd is used for plane wave expansion, and  $5 \times 5 \times 5$   $\mathbf{k}$ -mesh for integrations over the Brillouin zone. To account for the strong electron correlations, GGA+U (the generalized gradient approximation [8] plus Hubbard  $U$ ) calculations [9] were performed.  $U=5.0$  (4.0) eV for the Co (Mn)  $3d$  electrons (with a common Hund exchange of 0.9 eV) are used, according to the calculations using a local-orbital basis [10]. Note also that the choices of  $U$  value in the range of 2-7 eV do not affect the conclusion made in this Letter. The spin-orbit coupling (SOC) turns out to be crucial and it is included by the second-variational method with scalar relativistic wave functions [6].

It is quite common that an octahedral  $\text{Co}^{3+}$  ion is in a LS ground state. This may suggest that the small moment of  $0.66 \mu_B/\text{Co}$  in  $\text{Ca}_3\text{CoMnO}_6$  could be due to the Co/Mn site disorder, i.e., an appreciable presence of the octahedral LS  $\text{Co}^{3+}$ . To probe the Co/Mn site preference, we computed two structures either with the trigonal Co ( $\text{Co}_{\text{trig}}$ ) and octahedral Mn ( $\text{Mn}_{\text{oct}}$ ) or vice versa. The total energy results show that the former structure is more stable than the later by 0.33 eV/f.u. in GGA and more significantly, by 1.60 eV/f.u. in GGA+U+SOC. The energetically favorable structure has the HS trigonal  $\text{Co}^{2+}$  and the HS octahedral  $\text{Mn}^{4+}$ , while the unfavorable one indeed has the LS octahedral  $\text{Co}^{3+}$  and the HS trigonal  $\text{Mn}^{3+}$ . We plot in Fig. 1 the GGA and GGA+U+SOC calculated density of states (DOS) only for the favorable structure. The sharp DOS peak at the Fermi level, coming from the degenerate  $x^2-$

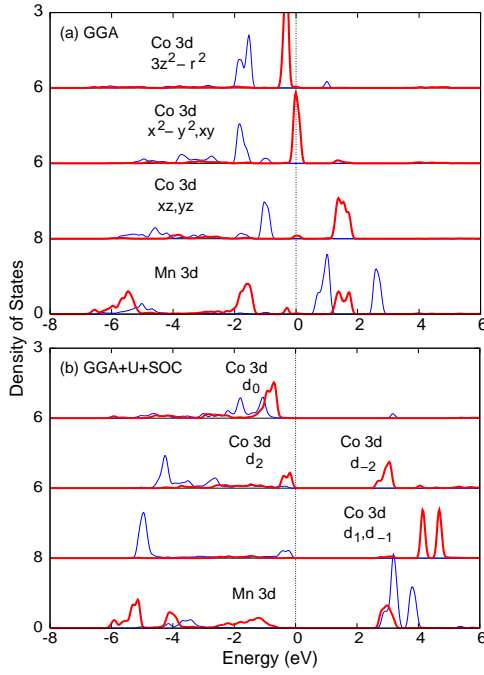


FIG. 1: (Color online) Density of states calculated by GGA (a) and GGA+U+SOC (b) for the  $\uparrow\uparrow\downarrow\downarrow$  spin structure of  $\text{Ca}_3\text{CoMnO}_6$  with the trigonal Co and octahedral Mn. It practically coincides with that for  $\uparrow\uparrow\downarrow\downarrow$ . The thin blue (bold red) curves refer to the majority (minority) spin. The Fermi level is set at zero energy. In (a) the  $\text{Mn}^{4+}_{\text{oct}}$  has a closed  $t_{2g}^3$  shell centered at  $-1.5$  eV, together with the  $e_g$  bonding state around  $-5.5$  eV. The  $\text{Co}_{\text{trig}}$  is in the high-spin  $2+$  state with the nearly degenerate  $3z^2-r^2$  ( $d_0$ ),  $x^2-y^2$  and  $xy$  ( $d_{\pm 2}$ ) levels. In (b) the  $(x^2-y^2, xy)$  doublet splits due to the spin-orbit coupling, and the Hubbard  $U$  yields an insulating ground state with the minority-spin  $d_0d_2$  occupation.

$y^2$  and  $xy$  ( $d_{\pm 2}$ ) levels of the trigonal  $\text{Co}^{2+}$  minority-spin  $d$  electrons, vanishes when going from the GGA to GGA+U+SOC solutions. This explains why, by opening a sizable gap of  $2.4$  eV, the GGA+U+SOC strongly favors the structure with the  $\text{Co}^{2+}_{\text{trig}}$  and  $\text{Mn}^{4+}_{\text{oct}}$ . The HS  $\text{Co}^{2+}$  ( $\text{Mn}^{4+}$ ) has a calculated spin moment of  $2.64$  ( $2.70$ )  $\mu_B$ , both staying constant within  $0.2 \mu_B$  for  $U=2-7$  eV.

Having established the  $\text{Co}^{2+}_{\text{trig}}/\text{Mn}^{4+}_{\text{oct}}$  site preference from the above total-energy calculations, we turn to our XAS measurements to confirm it. The room temperature Co- $L_{2,3}$  and Mn- $L_{2,3}$  XAS of  $\text{Ca}_3\text{CoMnO}_6$  were collected at the ID08 beamline of the European Synchrotron Radiation Facility (ESRF) in Grenoble with a resolution of  $0.25$  eV at Co- $L_3$  (at  $780$  eV). The sharp peak at  $777.8$  eV of the Co- $L_3$  edge of single crystalline CoO and at  $640$  eV of the Mn- $L_3$  of single crystalline MnO were used for energy calibration. The spectra were recorded using the total electron yield method by measuring the sample drain current in a chamber with a base pressure of  $2 \times 10^{-10}$  mbar. Clean sample areas were obtained by cleaving the polycrystals *in situ*.

Important is that XAS spectra are highly sensitive to

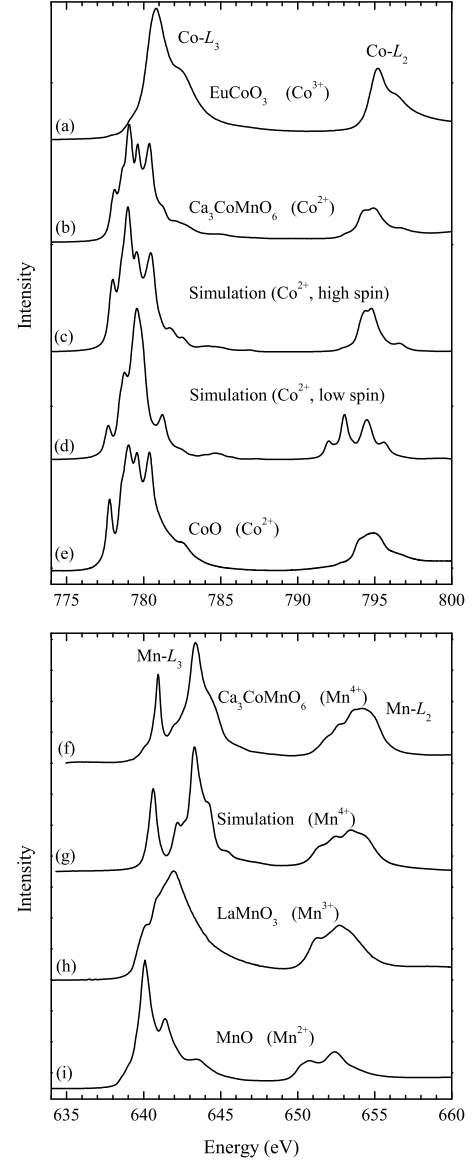


FIG. 2: The experimental and simulated x-ray absorption spectra of  $\text{Ca}_3\text{CoMnO}_6$  at the Co- $L_{2,3}$  (upper panel) and the Mn- $L_{2,3}$  (lower panel) edges, together with the experimental spectra of the references CoO,  $\text{EuCoO}_3$ , MnO, and  $\text{LaMnO}_3$ .  $\text{Ca}_3\text{CoMnO}_6$  turns out to have the high-spin trigonal  $\text{Co}^{2+}$  and octahedral  $\text{Mn}^{4+}$ .

the valence state: an increase of the valence state of the transition metal ion by one causes a shift of the XAS  $L_{2,3}$  spectra by one or more eV towards higher energies [11, 12]. In Fig. 2 (upper panel) we see a shift of the center of gravity of the Co- $L_3$  white line to higher photon energies by about  $1.5$  eV in going from the divalent CoO to the trivalent  $\text{EuCoO}_3$ . The energy position of the Co line in  $\text{Ca}_3\text{CoMnO}_6$  is the same as in CoO, indicating a  $\text{Co}^{2+}$  state. Also, a gradual shift of the center of gravity of the Mn- $L_3$  white line to higher energies from MnO via  $\text{LaMnO}_3$  to  $\text{Ca}_3\text{CoMnO}_6$  (lower panel in Fig. 2) evidences the increase of the Mn valence state from  $2+$  via  $3+$  to  $4+$ . In fact the Mn- $L_{2,3}$

edges of  $\text{Ca}_3\text{CoMnO}_6$  lie at the same energy position as in  $\text{SrMnO}_3$ ,  $\text{LaMn}_{0.5}\text{Co}_{0.5}\text{O}_3$  [12], and  $\text{LaMn}_{0.5}\text{Ni}_{0.5}\text{O}_3$  [13], all of which have the  $\text{Mn}^{4+}$  state. Thus, our XAS results confirm the  $\text{Co}^{2+}\text{-Mn}^{4+}$  state.

To extract more detailed information concerning the charge and spin states from the  $\text{Co-}L_{2,3}$  and the  $\text{Mn-}L_{2,3}$  XAS spectra, we have carried out simulations of the XAS spectra using the well-proven configuration-interaction cluster model [14, 15, 16]. We studied a trigonal prism  $\text{CoO}_6$  (an octahedral  $\text{MnO}_6$ ) cluster, including the full atomic multiplet theory and the local effects of the solid. Thus our model calculations account for the intra-atomic  $3d\text{-}3d$  and  $2p\text{-}3d$  Coulomb interactions, the atomic  $2p$  and  $3d$  spin-orbit couplings, the O  $2p\text{-Co } 3d$  hybridization, and the proper local crystal-field parameters. The calculated  $\text{Co-}L_{2,3}$  XAS spectrum for the HS  $\text{Co}^{2+}$  [curve (c) in Fig. 2] with the ionic trigonal crystal field interaction  $\Delta_{10}^{\text{ionic}}=0.75$  eV reproduces the experimental spectrum [curve (b)] very well [17]. In order to stabilize a LS state which was concluded by Choi *et al* [3], we would have to increase the  $\Delta_{10}^{\text{ionic}}$  by nearly 3 times (2.8 eV), and the calculated spectrum for this case [curve (d) in Fig. 2] strongly disagrees with the experimental one [curve (b)].

In the lower panel of Fig. 2, one can see that the lineshapes of the experimental Mn spectrum [curve (f)] are well reproduced by the simulation [curve (g)] with a  $\text{Mn}^{4+}$  ( $t_{2g}^3$ ) configuration in a local  $\text{O}_h$  symmetry.

Thus, our *ab initio* calculations and XAS experiments have firmly established that the spin-chain magnet  $\text{Ca}_3\text{CoMnO}_6$  has the HS  $\text{Co}_{\text{trig}}^{2+}$  and HS  $\text{Mn}_{\text{oct}}^{4+}$ , and that there is no appreciable presence of the LS- $\text{Co}_{\text{trig}}^{3+}/\text{HS-Mn}_{\text{trig}}^{3+}$ . Obviously, the magnetic moment of  $0.66 \mu_B/\text{Co}$  measured by neutron diffraction [3] below  $T_N \approx 13$  K is much smaller than our theoretical value [the total calculated moment being about  $4.3 \mu_B/\text{Co}$  with the spin (orbital) contribution of 2.6 (1.7)  $\mu_B$ , see more below] and than the value of  $\mu_{\text{eff}}=5.8\text{-}6.0 \mu_B$  obtained from the high-temperature magnetic susceptibility [4, 5]. This may be partially due to strong fluctuations in quasi one-dimensional chains, with frustrated interchain interactions. Another important factor may be a close proximity of different types of magnetic orderings, see below. This question deserves further study.

As seen in Fig. 1(a), the trigonal  $\text{Co}^{2+}$  has the nearly degenerate  $3z^2-r^2$  and  $(x^2-y^2, xy)$  levels. Due to the in-plane character of both the  $x^2-y^2$  and  $xy$  orbitals, their strong Coulomb repulsion prevents their double occupation in the minority-spin channel. Therefore, the minority-spin  $3z^2-r^2$  orbital is fully occupied and the minority-spin  $x^2-y^2$  and  $xy$  are half-filled for the HS  $\text{Co}^{2+}$  ions. Due to the quasi one-dimensional character along the  $c$ -axis chain, a naive  $x^2-y^2/xy$  planar orbital ordering does not gain any energy (compared with either an  $x^2-y^2/x^2-y^2$  or  $xy/xy$  orbital ordering), as proved by our *ab initio* calculations. In contrast, an efficient way to

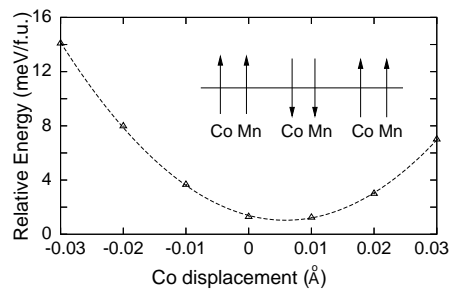


FIG. 3: Relative energy as function of the Co displacements calculated by GGA+U+SOC for the experimental lattice. Triangles stand for the data points, which are fitted into a parabolic curve. The energy minimum shows the Co displacement of 0.006 Å, which leads to alternate short-long-short-long Co-Mn distances (the difference being 0.012 Å) in the  $\text{Co}\uparrow\text{-Mn}\uparrow\text{-Co}\downarrow\text{-Mn}\downarrow$  chain as depicted schematically in inset.

gain the energy is SOC. When the SOC is included, the  $(x^2-y^2, xy)$  doublet splits into  $d_2$  and  $d_{-2}$ , and the gain of the full SOC energy is calculated to be about 70 meV. As a result, a huge orbital magnetic moment of  $1.7 \mu_B$  is generated at the HS  $\text{Co}_{\text{trig}}^{2+}$  sites with the minority-spin  $d_0d_2$  occupation [Fig. 1(b)], and the SOC firmly fixes the total magnetization (with parallel spin and orbital contributions) along the  $c$ -axis chain direction. Note that the orbital moment stays constant within  $0.1 \mu_B$  in our GGA+U+SOC calculations for  $U=2\text{-}7$  eV. Therefore, the peculiar trigonal crystal field and the SOC are responsible for the significant Ising character of  $\text{Ca}_3\text{CoMnO}_6$ ; cf. similar situation in the isostructural  $\text{Ca}_3\text{CoRhO}_6$  [19].

Having established the picture about the Co/Mn site preference, their charge/spin/orbital states and the significant Ising magnetism, we turn now to the discussion on the intra-chain magnetism and the exchange striction leading to ferroelectricity. Since a centrosymmetric structure of  $\text{Ca}_3\text{CoMnO}_6$  does not carry ferroelectricity, we now look whether the symmetry can be lowered by allowing for atomic displacements within the *experimentally observed* [3]  $\uparrow\uparrow\downarrow\downarrow$  magnetic structure of the Co-Mn-Co-Mn Ising spin chain: the Co-Mn bonds would be inequivalent in such a non-centrosymmetric structure leading to chain dimerization, and this will give rise to ferroelectricity. We calculated using GGA+U+SOC the total energy of the system by firstly shifting the Co ions along the chain making Co-Mn distances unequal (alternating) [20]. The results are shown in Fig. 3. We see that indeed the lattice in  $\uparrow\uparrow\downarrow\downarrow$  structure would relax to a state with alternating Co-Mn distances (the difference being 0.012 Å), which means the appearance of FE in the system, cf. [21, 22, 23, 24]. The calculated spin and orbital moments remain unchanged. Furthermore, a triclinic lattice ( $P1$ ) was tested to study a likely breaking of the 3-fold rotation symmetry. A structural relaxation using GGA+U+SOC (with the Co ions fixed at the above optimized position) confirms the small FE distortion of the Co-Mn chains and gives also a small distortion of the Co-O (Mn-O) bonds

[only about 0.01 Å out of 2.15 Å (1.92 Å) in bondlength]. We would like to point out that those small distortions are not inconsistent with the experiment [7] since they are so small that they would require a special effort for their detection.

We note that in the GGA+U+SOC calculations the  $\uparrow\uparrow\downarrow\downarrow$  and  $\uparrow\downarrow\uparrow\downarrow$  magnetic structures for the Co-Mn-Co-Mn spin chain are the two lowest-energy states, with the former being higher in energy. The energy difference is 15 meV/f.u. for the experimentally detected crystal structure [4] and is reduced to 7 meV/f.u. for the relaxed triclinic lattice (*P*1). At the moment it is not clear how to stabilize the experimentally observed  $\uparrow\uparrow\downarrow\downarrow$  magnetic structure [3] in the GGA+U+SOC calculations. Since the energy difference is rather small and the intrachain exchange interactions rather weak, we speculate that the couplings between the chains may play an important role. The present calculations assumed a simple ferromagnetic interchain interaction, but it is known that there are AF interchain couplings in the isostructural  $\text{Ca}_3\text{Co}_2\text{O}_6$  [25] and  $\text{Ca}_3\text{CoRhO}_6$  [26] compounds with strengths not much smaller than the intrachain ones. These finite AF interchain couplings bring about magnetic frustration, and one needs to investigate a large set of intra- and interchain magnetic structures in order to explain theoretically the magnetic ground state of  $\text{Ca}_3\text{CoMnO}_6$ .

In summary, we find the site preference of the high-spin trigonal  $\text{Co}^{2+}$  and the octahedral  $\text{Mn}^{4+}$  in the Ising chain magnet  $\text{Ca}_3\text{CoMnO}_6$ , using the *ab initio* calculations and x-ray absorption spectroscopy. The  $\text{Co}^{2+}$  has the very stable minority-spin  $d_0d_2$  occupation due to the peculiar trigonal crystal field, inter-orbital Coulomb repulsion and the spin-orbit coupling. Thus, a huge orbital moment of  $1.7 \mu_B$  is predicted and the significant Ising magnetism is well accounted for. Moreover, our calculations indeed found that a structural relaxation due to the exchange striction decreases the energy of the experimentally observed  $\uparrow\uparrow\downarrow\downarrow$  magnetic ordering and leads to the observed ferroelectricity. However, the mechanism of the full stabilization of the  $\uparrow\uparrow\downarrow\downarrow$  structure as the ground state calls for a further study.

We are grateful to V. Kiryukhin and S. W. Cheong for informing us of their unpublished structural data. This research was supported by the Deutsche Forschungsgemeinschaft through SFB 608.

- 
- [1] S. W. Cheong and M. Mostovoy, *Nat. Mater.* **6**, 13 (2007).
  - [2] D. I. Khomskii, *J. Magn. Magn. Mater.* **306**, 1 (2006).
  - [3] Y. J. Choi, H. T. Yi, S. Lee, Q. Huang, V. Kiryukhin, and S. W. Cheong, *Phys. Rev. Lett.* **100**, 047601 (2008).

- [4] V. G. Zubkov, G. V. Bazuev, A. P. Tyutyunnik, and I. F. Berger, *J. Solid State Chem.* **160**, 293 (2001).
- [5] S. Rayaprol, K. Sengupta, and E. V. Sampathkumaran, *Solid State Commun.* **128**, 79 (2003).
- [6] P. Blaha, K. Schwarz, G. Madsen, D. Kvasnicka, and J. Luitz, Wien2k package, <http://www.wien2k.at>
- [7] V. Kiryukhin and S. W. Cheong (private communication). Their neutron diffraction measurements at 1.4 K gave practically coinciding structure data with the room-temperature data in Ref. 4: No symmetry lower than the *R*-3c was observed, and the ferroelectric distortion is too small to be detected.
- [8] J. P. Perdew, K. Burke, and M. Ernzerhof, *Phys. Rev. Lett.* **77**, 3865 (1996).
- [9] V. I. Anisimov, I. V. Solovyev, M. A. Korotin, M. T. Czyżyk, and G. A. Sawatzky, *Phys. Rev. B* **48**, 16929 (1993).
- [10] W. E. Pickett, S. C. Erwin, and E. C. Ethridge, *Phys. Rev. B* **58**, 1201 (1998).
- [11] C. Mitra, Z. Hu, P. Raychaudhuri, S. Wirth, S. I. Csiszar, H. H. Hsieh, H.-J. Lin, C. T. Chen, and L. H. Tjeng, *Phys. Rev. B* **67**, 092404 (2003).
- [12] T. Burnus, Z. Hu, H. H. Hsieh, V. L. J. Joly, P. A. Joy, M. W. Haverkort, H. Wu, A. Tanaka, H.-J. Lin, C. T. Chen, and L. H. Tjeng, *Phys. Rev. B* **77**, 125124 (2008).
- [13] M. C. Sánchez, J. García, J. Blasco, G. Subías, and J. Perez-Cacho, *Phys. Rev. B* **65**, 144409 (2002).
- [14] A. Tanaka and T. Jo, *J. Phys. Soc. Jpn.* **63**, 2788 (1994).
- [15] F. M. F. de Groot, *J. Electron Spectrosc. Rel. Phenom.* **67**, 529 (1994).
- [16] See the “Theo Thole Memorial Issue”, *J. Electron Spectrosc. Rel. Phenom.*, **86**, 1 (1997).
- [17] Parameters (in eV). Co:  $U_{3d3d} = 5$ ,  $U_{2p3d} = 6.5$ ,  $\Delta = 4$ ,  $\Delta_{10}^{\text{ionic}} = 0.75$  (HS),  $\Delta_{10}^{\text{ionic}} = 2.8$  (LS),  $\Delta_{20}^{\text{ionic}} = -0.1$ ,  $V_{\text{mix}}^{\text{ionic}} = 0.15$ . Hybridization from Harrison’s rules (Ref. 18). Mn:  $U_{3d3d} = 5$ ,  $U_{2p3d} = 6$ ,  $\Delta = -3$ ,  $\Delta_{\text{CF}} = 2$ ,  $V_{pd\sigma} = -1.6$ . The Slater integrals were reduced to 80% (for Co) and 70% (for Mn) of their Hartree-Fock value.
- [18] W. A. Harrison, *Electronic Structure and the Properties of Solids*, Dover (1989).
- [19] H. Wu, Z. Hu, D. I. Khomskii, and L. H. Tjeng, *Phys. Rev. B* **75**, 245118 (2007).
- [20] Co ions are in the relatively open trigonal prisms, compared with Mn in the octahedra. Thus, Co is more susceptible to the exchange striction, as proved by the structural relaxation.
- [21] D. V. Efremov, J. van den Brink, and D. I. Khomskii, *Nature Materials* **3**, 853 (2004).
- [22] S. Picozzi, K. Yamauchi, B. Sanyal, I. A. Sergienko, and E. Dagotto, *Phys. Rev. Lett.* **99**, 227201 (2007).
- [23] H. J. Xiang, S. H. Wei, M. H. Whangbo, and J. L. F. Da Silva, *Phys. Rev. Lett.* **101**, 037209 (2008).
- [24] J. van den Brink, and D. I. Khomskii, *J. Phys.: Condens. Matter*, in press, (cond-mat/arXiv:0803.2964).
- [25] H. Kageyama, K. Yoshimura, K. Kosuge, H. Mitamura, and T. Goto, *J. Phys. Soc. Jpn.* **66**, 1607 (1997).
- [26] S. Niitaka, K. Yoshimura, K. Kosuge, M. Nishi, and K. Kakurai, *Phys. Rev. Lett.* **87**, 177202 (2001).